Wood Science and Technology (2020) 54:1241–1251
https://doi.org/10.1007/s00226-020-01209-x

ORIGINAL

# Time domain-NMR studies of average pore size of wood cell walls during drying and moisture adsorption

**Xinyu Li**[1] · **Zhihong Zhao**[2]

Received: 25 January 2020 / Published online: 5 August 2020


## Abstract

The change in the pore size of cell walls affects many physical properties of wood. In this paper, the dynamic changes in the pore size of wood cell walls during drying and moisture adsorption were studied at four relative humidities. The results showed that the average pore size of cell walls of Qingpi poplar (*Populus- platyphylla* var. *glauca*) was larger than that of pine wood (*Pinus sylvestris* var. *mongolica* Litv.) under the same experimental conditions, and the changes in pore size of Qingpi poplar cell walls were more sensitive to ambient humidity no matter whether during drying or moisture adsorption. Moreover, the average pore size of cell walls at saturated-water state is about 2.5 times of the average pore size of cell walls when woods reached the moisture absorption equilibrium from the oven-dry state. This article is useful for the wood manufacture industry and for wood modification. It is not only important for wood processing and utilization but also for the research on other porous materials.

## Introduction

Wood is widely used in furniture and building industry, although it is easily affected by the change in moisture content (MC). It is generally believed that below the fiber saturation point (FSP), the moisture molecules combine with wood by hydrogen bonds. Representative theories of moisture adsorption are the monomolecular layer adsorption theory and the multimolecular layer adsorption theory. The former is represented by the Langmuir theory (Hailwood and Horrobin 1946: Langmuir 1918) and the latter by the BET (Brunauer, Emmett and

✉ Xinyu Li
826249963@qq.com

Zhihong Zhao
1197428998@qq.com

[1] Institute of Carbon Materials Science, Shanxi Datong University, Datong 037009, China

[2] College of Materials Science and Art Design, Inner Mongolia Agricultural University, Hohhot 010018, China

Teller) theory (Brunauer et al. 1938) and the Polanyi adsorption potential theory (Dubinin 1966). The pore size of cell walls shrinks with drying and increases with moisture adsorption, which has a great impact on the macrosize and physical properties of wood. Hence, the study of wood pore size is important for wood modification and wood building industry.

The International Union of Pure and Applied Chemistry (IUPAC) classified the pore size of porous materials into micropores (< 2 nm), mesopores (2–50 nm) and macropores (> 50 nm) (Everett 2009). Many methods have been proposed to study the pore size, some of which are also applicable to wood. Mercury intrusion porosimetry is an effective way for macropore measurement in wood (Vitas et al. 2019). However, the wood sample needs to be dried, and during mercury intrusion, the pore structure might be destroyed. Gas adsorption isotherms are capable of detecting micropores and mesopores (Yang and Tze 2017; Yin et al. 2015). However, for the traditional $N_2$ adsorption, the wood sample needs to be dried and conducted at a low temperature (< −196 °C), which potentially affects the wood's microstructure. In the water vapor sorption detection (Driemeier et al. 2012; Grönquist et al. 2019), the original cell wall nanostructure can be retained since the wood is not completely dried, but it is not time-saving enough. Scanning electron microscopy (Galmiz et al. 2019) could offer comprehensive information on the pore structure, but the preparation of samples is complex and the field of vision is small, and even worse, only partial information on pore materials could be obtained. Besides, small-angle X-ray scattering (Kalliat et al. 1983; Penttilä et al. 2019) and atomic force microscopy (Hanley and Gray 2009) were also used for pore size detection, but inevitably, the sample flatness will greatly affect the results.

In comparison, time domain-nuclear magnetic resonance (TD-NMR) technique has attracted much attention in the study of porous materials due to its non-destructive and efficient advantages (Adebayo et al. 2017; Ghomeshi et al. 2018; Li et al. 2015; Meyer et al. 2015). Nowadays, it is affirmed to be efficient in studying the pore size of wood-based materials. Gao et al. (2015) studied the pore size distribution in swollen cell walls of wood by nuclear magnetic resonance (NMR) cryoporometry. Their results showed that the proportion of pores smaller than 1.59 nm was more than 70%, and the proportion of the pore diameter larger than 4 nm was no more than 10%. The NMR cryoporometry and relaxometry analyses of thermally modified pine wood (*Pinus sylvestris*) (Kekkonen et al. 2014) indicated that the sizes of bound water sites are mostly below 2.5 nm in both thermally modified and unmodified pine wood. Besides, the size of cell wall micropores is between 1.5 and 4.5 nm (Kekkonen et al. 2014). The TD-NMR was also applied to the determination of the average pore size and distribution in an ancient larch wood (Viel et al. 2004), and the results revealed that the average dimension of the pores was about 1 nm and the distribution was found to be strongly asymmetric.

Although the pore size of wood has already been investigated by TD-NMR technique, there are few studies available on investigating the dynamic change in the pore size during drying and moisture adsorption. The change in pore size has a big influence on the wood properties, which is very important not only for the wood manufacture industry but also in wood modification.

## Materials and methods

### Materials

Two kinds of fresh wood, Qingpi poplar and *P. sylvestris*, were used in this experiment, and both of them were harvested from the surrounding areas of Hohhot, Inner Mongolia of China, with an approximate age of 10 years. The specimens were cylindrical with the dimension of 12 mm ($\Phi$) × 20 mm ($L$). All specimens were drilled from the xylem of the sapwood parallel to the fiber direction, and 4 specimens for each kind of wood were obtained.

Four kinds of SBA-15 molecular sieves with an average pore size of 0.3 nm, 1 nm, 2.67 nm and 4.78 nm (Nanjing Jicang Nano Technology Co., Ltd) were used for NMR-$T_2$ (spin–spin relaxation time) measurements to establish the standard curve between $T_2$ relaxation time and pore size.

Four kinds of analytical grade salts (Tianjin Beilian Fine Chemicals Development Co., Ltd), including magnesium chloride ($MgCl_2$), sodium bromide (NaBr), sodium nitrate ($NaNO_3$) and potassium sulfate ($K_2SO_4$), were used to prepare saturated salt solutions to obtain different relative humidities during drying and moisture adsorption.

## Experimental methods

### $T_2$ measurement of molecular sieves

The SBA-15 molecular sieves were firstly water-saturated at room temperature and then detected for the NMR-$T_2$ measurements using a TD-NMR spectrometer (Bruker Minispec mq 20 NMR spectrometer, Bruker Corporation, Karlsruhe, Germany). The console operated at 19.95 MHz inside the magnetic body at a constant temperature of 40 °C; the probe diameter was 18 mm, and the dead time was 4.5 μs. A CPMG (Carr–Purcell–Meiboom–Gill) sequence was used for the $T_2$ measurement, with a 90° pulse width of 14.94 μs and a 180° pulse width of 30.5 μs; the number of scans was 8; the cycle delay was 2 s; 200 echoes were used with the half echo time of 0.1 ms.

### $T_2$ measurement of water in wood during drying and moisture adsorption

Firstly, four kinds of saturated salt solution were prepared and then poured into four desiccators, each solution with the addition of a small amount of corresponding salt to make it supersaturated. In addition, a thermohygrograph (white disk in the desiccator as shown in Fig. 1) was placed in each desiccator to record the internal temperature and humidity. To prevent the wood specimens from falling into the salt solutions, a piece of plastic gauze was placed on the magnetic holder.

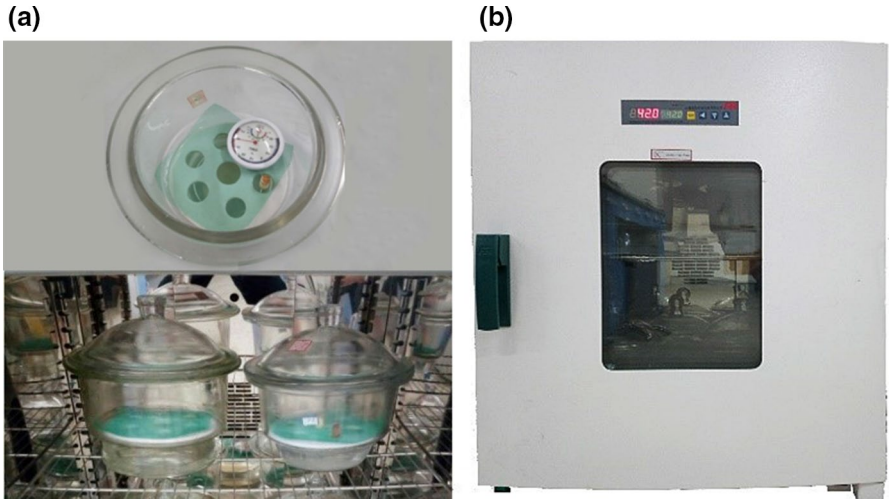


**Fig. 1** Equipment for wood drying. The desiccator with saturated salt solution at the bottom and a thermohygrograph and wood sample on the stand (top left); four desiccators as described in **a** placed in the drying oven (bottom left); the working drying oven (right) (**b**)

The wood samples were dried at a relatively low temperature of 40 °C at four different relative humidities via a drying oven as shown in Fig. 1.

Four desiccators were heated in a drying oven at 42 °C (the temperature inside desiccators is about 40 °C, as recorded by thermohygrograph) for 24 h so that the temperature and relative humidity inside the desiccators could reach the experimental conditions. The relative humidities of the four saturated salt solutions at 40 °C according to OIML R 121 (standard relative humidity value of saturated salt solution) are shown in Table 1.

Prior to the $T_2$ measurements, all specimens were firstly immersed in distilled water for water saturation, in a vacuum (− 0.084 MPa) for 24 h at room temperature, so as to ensure all pores in the wood were water-saturated. In doing so, the $T_2$ signal of water, in particular the bound water in wood during drying and moisture adsorption, was detected.

During the drying process, the water-saturated specimens of each type of wood were dried under different relative humidities in four desiccators. After different drying intervals, the specimens were taken out of the desiccators and placed into the nuclear magnetic probe for NMR $T_2$ measurements. The $T_2$ measurements were taken by using a CPMG (Carr–Purcell–Meiboom–Gill) sequence; the

**Table 1** Relative humidity of five kinds of saturated salt solutions at 40 °C

| Saturated salt solutions | $MgCl_2$ | NaBr | $NaNO_3$ | $K_2SO_4$ |
|---|---|---|---|---|
| Temperature (°C) | 40 | | | |
| Relative humidity (%) | 31.6 | 53.2 | 71 | 96.4 |

number of echoes was set at 6000, so as to acquire all water signals in wood, and the other parameters were the same as those for the determination of molecular sieves. For each specimen, multiple $T_2$ measurements were required during the entire drying process at the respective relative humidity, the intervals between each $T_2$ measurement being gradually increased with drying. When the weight change was less than 0.1% of the last weight after 48 h, it was considered that the equilibrium moisture content (EMC) was reached and the drying process was accomplished, and hence, the $T_2$ measurements of drying were taken. Finally, all specimens were oven-dried at 105 °C for 24 h.

After the drying procedure, all oven-dried specimens were put into the same desiccators for moisture adsorption at room temperature, and the $T_2$ signals of adsorbed water in wood were acquired during the moisture adsorption. Similar to the $T_2$ measurement of the drying procedure, multiple $T_2$ measurements were also required during the entire moisture adsorption at the respective relative humidity for each specimen, the intervals between each $T_2$ measurement being gradually increased with moisture adsorption. $T_2$ measurements were taken until the EMC was reached. The parameters were basically the same as those for the $T_2$ measurement of molecular sieves; the number of echoes was set at 100 due to the relatively low MC.

$T_2$ data were inversed by CONTIN arithmetic (Provencher 1982), and hence, the average pore size of cell walls during drying and adsorption was calculated by the inversion results.

## Results and discussion

### Calculation of the pore size

Generally, the $T_2$ relaxation of water in porous medium could be expressed as the sum of bulk relaxation, surface relaxation and diffusion relaxation (Durrett 1984; Toumelin et al. 2007):

$$\frac{1}{T_2} = \frac{1}{T_{2\mathrm{B}}} + \frac{1}{T_{2\mathrm{S}}} + \frac{D(\gamma G T_{\mathrm{E}})^2}{12} \tag{1}$$

where $\frac{1}{T_2}$ is the total $T_2$ relaxation rate, $\frac{1}{T_{2\mathrm{B}}}$ is the $T_2$ relaxation rate of bulk water, $\frac{1}{T_{2\mathrm{S}}}$ is the $T_2$ relaxation rate of water on the internal surface. $\frac{D(\gamma G T_{\mathrm{E}})^2}{12}$ is diffusion relaxation, $D$ is the diffusion coefficient of water in porous media, $\gamma$ is the gyromagnetic ratio of hydrogen nucleus, $G$ is external magnetic field gradient, herein, $G \approx 0$ Gs/cm since the external magnetic field is approximately uniform. $T_{\mathrm{E}}$ is echo time, here it is 0.1 ms. So $\frac{D(\gamma G T_{\mathrm{E}})^2}{12}$ can be ignored owing to its small value.

Usually, bulk water has a low relaxation efficiency, and there is no bulk water in wood; hence, $\frac{1}{T_{2\mathrm{B}}}$ in Eq. (1) could be ignored. Moreover, the interaction of solid–liquid interface accelerates the water relaxation, and the surface water contributes to the main relaxation (Li et al. 2015). In this case, Eq. (1) is simplified as:

$$\frac{1}{T_2} \approx \frac{1}{T_{2S}} = \rho\left(\frac{S}{V}\right) \tag{2}$$

where $\rho$ is the surface relaxivity, $S$ is surface area, $V$ is volume, $\frac{S}{V}$ is specific surface area. The $T_2$ relaxation of water in porous medium can usually be written as (He et al. 2005)

$$\frac{1}{T_2} = \rho\left(\frac{S}{V}\right) = \rho\frac{F_s}{r} \tag{3}$$

where $r$ is the pore diameter, and $F_s$ is the geometric shape factor. It is assumed that the pores in wood are all cylindrical pores; hence, $F_s = 2$ (He et al. 2005). The pore size is proportional to $T_2$ values as shown in Eq. (4):

$$T_2 = \frac{r}{2\rho} \tag{4}$$

The SBA-15 molecular sieves are taken as standard samples since they have hygroscopic and cylindrical pores, which is similar to wood. As shown in Fig. 2, there is a linear relationship between $T_2$ relaxation time and pore size. Here, the average pore size of wood cell walls is calculated during drying and moisture adsorption based on the linear fitting equation in Fig. 2.

## Changes in the pore size of cell walls during drying

Normally, free water mainly exists in the cell lumina, the change of its content only affects the mass of wood itself, and there are no evident structural changes when increasing the moisture content above the FSP (Jakob et al. 1996). The main proportion of bound water exists in $S_2$ layer of the secondary cell wall and is bound to

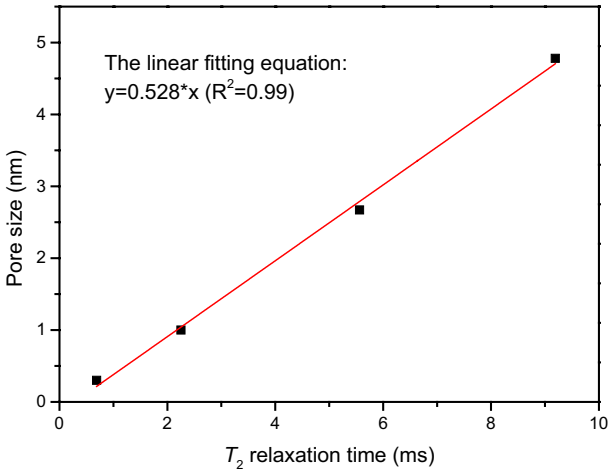


**Fig. 2** Relationship between $T_2$ relaxation time and pore size

hydroxyl groups of hemicelluloses and the surfaces of cellulose microfibrils (Hofstetter et al. 2006; Engelund et al. 2013). The change in moisture content results in the shrinkage and swelling of wood below FSP. During drying, the thermal energy accelerates the water firstly and then evaporates it out of the cell walls. The water-swollen polysaccharide matrix shrinks strongly, pulling the cellulose microfibrils closer to each other (Penttilä et al. 2020), which is the main reason for the change in the pore size of cell walls, even the macrosize of wood. Therefore, the decrease in bound water is the most important factor causing shrinkage.

Figure 3 shows the change in pore diameter of the cell wall during drying at different relative humidity. The calculation results of the pore size are in agreement with previous studies (Stamm 1967; Fengel 1970; Li et al. 1993; Grigsby et al. 2013). It can be seen that the average pore size of cell walls of Qingpi poplar is 2.2 times larger than that of *P. sylvestris* at the beginning of drying. The pore diameter of wood cell walls decreases with drying, the lower the relative humidity, the more thorough the wood drying, and therefore the smaller the average pore size of cell walls. For both kinds of wood, the increasing relative humidity slows down the decrease in pore size, but the differences in wood species led to a different humidity sensitivity. The changes in cell wall pore size of Qingpi poplar are more significantly affected by the change in relative humidity. In comparison, the change in the pore size of *P. sylvestris* is more sensitive to high relative humidity (96.4%). Moreover, for both wood species, the average pore size of the cell walls is basically equal when the relative humidities are 31.6% and 53.2%.

For both hardwood and softwood, the wood cell walls are composed of longitudinally oriented cellulose fibrils embedded within an amorphous hemicellulose and lignin matrix (Gibson 2012). Normally, the cellulose content is almost equal, but the hemicellulose content in hardwood is more than that in softwood, and the lignin content in softwood is more than that in hardwood. Qingpi poplar is a hardwood, and *P. sylvestris* is a softwood. The change in the pore size of cell walls shown in Fig. 3 is probably caused by the different content in hemicellulose and lignin. Compared with *P. sylvestris*, Qingpi poplar has a higher content of hemicellulose and

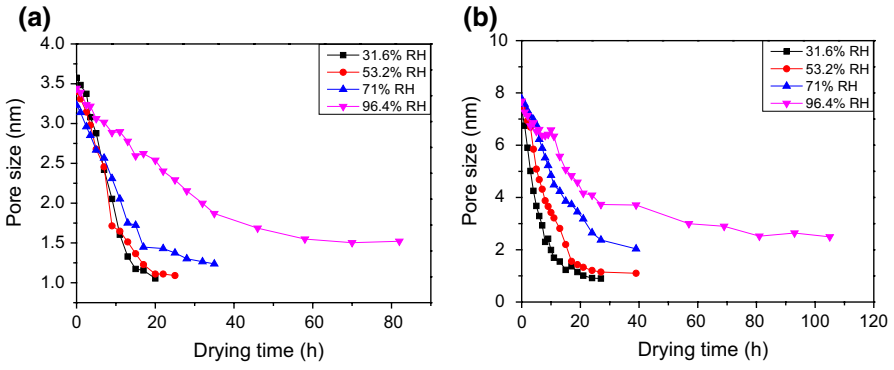


**Fig. 3** Pore size of *P. sylvestris* and Qingpi poplar during the drying process. **a** Change in pore size of *P. sylvestris* and **b** change in pore size of Qingpi poplar

less content of lignin. In this case, it has more sites to accommodate water molecules, the water molecules in the cell walls easily interact with water molecules in the surrounding environment, and hence the change in pore size of cell walls is more sensitive to the change in relative humidity. Furthermore, there is more lignin in *P. sylvestris*, which weakens the exchange of water molecules between wood cell walls and the ambient environment. Therefore, the change in the pore size of cell walls is only slowed down at the highest relative humidity.

### Changes in the pore size of cell walls during moisture adsorption

According to the BET (Brunauer–Emmett–Teller) adsorption theory, a few water molecules enter wood firstly and then bind to cell walls in a monomolecular layer; the subsequent water molecules combine with the absorbed water molecules forming a multimolecular layer. During the adsorption process, water molecules enter the cell walls, causing swelling of the material, occupying space between the microfibrils and thereby forcing them apart. Furthermore, the microfibrils themselves experience a change in dimension (Zabler et al. 2010; Toba et al. 2012), which changes the pore size of cell walls, and finally leads to the macroscopic swelling of wood (Murata and Masuda 2006). Figure 4 shows the change in the pore size of cell walls for both wood species, which agrees with a previous study (Lin et al. 1987).

Figure 4 shows the average pore size of cell walls was basically unchanged at 31.6% relative humidity and 53.2% relative humidity. It indicates that there are a few water molecules entering wood at this relative humidity, and it is not enough to wet the cell walls of the wood and cause it swelling. There is a small increase in the pore size of cell walls in *P. sylvestris* at the end of moisture adsorption since the relative humidity increases to 71%. Moreover, it is 10 h later when the pore size of the cell walls in Qingpi poplar is gradually increasing, yet for *P. sylvestris*, it is more than 30 h. Besides, there is a large increase in the pore size of cell walls at the highest relative humidity (96.4%). In comparison, the pore size of cell walls of Qingpi poplar is 2.4 times bigger than that of *P. sylvestris*. It is supposed that the different changes

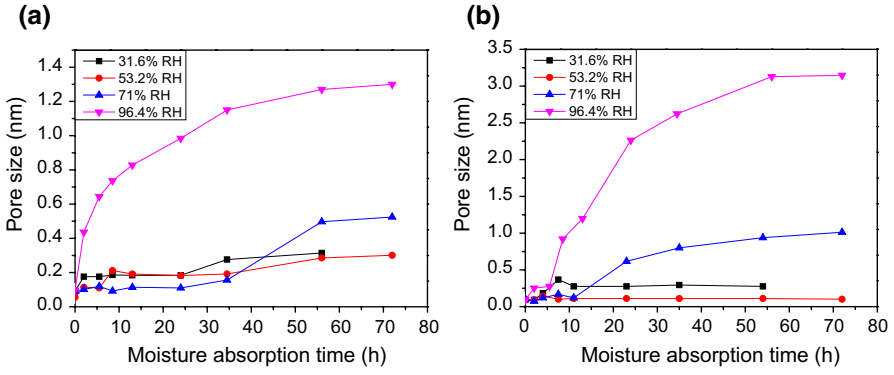


**Fig. 4** Pore size of *P. sylvestris* and Qingpi poplar during moisture adsorption process. **a** Change in the pore size of *P. sylvestris* and **b** change in the pore size of Qingpi poplar

in the pore size of cell walls derive from the differences in hemicellulose and lignin contents. Compared with Qingpi poplar, the pore size of *P. sylvestris* only shows a sensitivity to the highest humidity due to the higher lignin content; in other words, only when the concentration of water molecules in the environment is high enough, the water molecules will enter the wood cell walls and cause wood swelling.

In addition, the pore diameter of the cell walls of *P. sylvestris* at water-saturated state is about 2.6 times larger than when the oven-dried *P. sylvestris* achieves adsorption equilibrium. For Qingpi poplar, it is about 2.4 times larger. This is because when the wood is completely dried, most of the cell wall pores are closed. When the wood is wetted again, only parts of the cell wall pores could be reopened (Fengel 1970).

## Conclusion

The dynamic changes in the pore size of wood cell walls during drying and moisture adsorption at different relative humidities were studied, and the following conclusions are drawn

1. Whether at water-saturated state or at moisture adsorption equilibrium state at 96.4% relative humidity, the average pore size of cell walls of Qingpi poplar is about 2.2 times larger than that of *P. sylvestris*.
2. Compared with *P. sylvestris*, the change in the pore size of cell walls of Qingpi poplar is more sensitive to ambient humidity during drying and moisture adsorption.
3. For both wood species, the average pore size of the cell walls at saturated-water state is about 2.5 times that of the average pore size of cell walls when woods reached the moisture absorption equilibrium from oven-dry state.

**Acknowledgements** This research was supported by the Doctoral Scientific Research Foundation of Datong University (2018-B-16).

## References

Adebayo AR, Kandil ME, Okasha TM, Sanni ML (2017) Measurements of electrical resistivity, NMR pore size and distribution, and x-ray CT-scan for performance evaluation of CO2 injection in carbonate rocks: a pilot study. Int J Greenh Gas Control 63:1–11. https://doi.org/10.1016/j.ijggc.2017.04.016

Brunauer S, Emmett PH, Teller E (1938) Adsorption of gases in multimolecular layers. J Am Chem Soc 60:309–319. https://doi.org/10.1021/ja01269a023

Driemeier C, Mendes FM, Oliveira MM (2012) Dynamic vapor sorption and thermoporometry to probe water in celluloses. Cellulose 19:1051–1063. https://doi.org/10.1007/s10570-012-9727-z

Dubinin MM (1966) Porous structure and adsorption properties of active carbons. Chem Phys Carbon 2:51–120

Durrett R (1984) Oriented percolation in two dimensions. Ann Probab 12:999–1040

Engelund ET, Thygesen LG, Svensson S, Hill CAS (2013) A critical discussion of the physics of wood–water interactions. Wood Sci Technol 47:141–161. https://doi.org/10.1007/s00226-012-0514-7

Everett DH (2009) Manual of symbols and terminology for physicochemical quantities and units, appendix II: definitions, terminology and symbols in colloid and surface chemistry. Pure Appl Chem 31:577–638. https://doi.org/10.1351/pac197231040577

Fengel D (1970) The ultrastructure of cellulose from wood-Part 2: problems of the isolation of cellulose. Wood Sci Technol 4:15–35. https://doi.org/10.1007/bf00356234

Galmiz O, Talviste R, Panček R, Kovčik D (2019) Cold atmospheric pressure plasma facilitated nanostructuring of thermally modified wood. Wood Sci Technol 53:1339–1352. https://doi.org/10.1007/s00226-019-01128-6

Gao X, Zhuang S, Jin J, Cao P (2015) Bound water content and pore size distribution in swollen cell walls determined by NMR technology. BioResour 10:8208–8224. https://doi.org/10.15376/biores.10.4.8208-8224

Ghomeshi S, Kryuchkov S, Kantzas A (2018) An investigation into the effects of pore connectivity on $t_2$ nmr relaxation. J Magn Reson 289:79–91. https://doi.org/10.1016/j.jmr.2018.02.007

Gibson LJ (2012) The hierarchical structure and mechanics of plant materials. J R Soc Interface 9:2749–2766. https://doi.org/10.1098/rsif.2012.0341

Grigsby WJ, Kroese H, Dunningham EA (2013) Characterisation of pore size distributions in variously dried Pinus radiata: analysis by thermoporosimetry. Wood Sci Technol 47:737–747. https://doi.org/10.1007/s00226-013-0537-8

Grönquist P, Frey M, Keplinger T, Burgert I (2019) Mesoporosity of delignified wood investigated by water vapor sorption. Acs Omega 4:12425–12431. https://doi.org/10.1021/acsomega.9b00862

Hailwood AJ, Horrobin S (1946) Absorption of water by polymers: analysis in terms of a simple model. Trans Faraday Soc 42:84–92. https://doi.org/10.1039/tf946420b084

Hanley SJ, Gray DG (2009) Atomic force microscope images of black spruce wood sections and pulp fibres. Holzforschung 48:29–34. https://doi.org/10.1515/hfsg.1994.48.1.29

He Y, Mao Z, Xiao L, Ren X (2005) An improved method of using NMR $T_2$ distribution to evaluate pore size distribution. Chin J Geophys Chin Ed 48:373–378. https://doi.org/10.3321/j.issn:0001-5733.2005.02.020

Hofstetter K, Hinterstoisser B, Salmén L (2006) Moisture uptake in native cellulose-the roles of different hydrogen bonds: a dynamic FT-IR study using deuterium exchange. Cellulose 13:131–145. https://doi.org/10.1007/s10570-006-9055-2

Jakob HF, Tschegg SE, Fratzl P (1996) Hydration dependence of the wood-cell wall structure in *Picea abies*. A small-angle X-ray scattering study. Macromolecules 29:8435–8440. https://doi.org/10.1021/ma9605661

Kalliat M, Kwak CY, Schmidt PW, Cutter BE, Mcginnes EA (1983) Small angle X-ray scattering measurement of porosity in wood following pyrolysis. Wood Sci Technol 17:241–257. https://doi.org/10.1007/bf00349913

Kekkonen PM, Ylisassi A, Telkki V-V (2014) Absorption of water in thermally modified pine wood as studied by nuclear magnetic resonance. J Phys Chem C 118:2146–2153. https://doi.org/10.1021/jp411199r

Langmuir I (1918) The adsorption of gases on plane surfaces of glass, mica and platinum. J Am Chem Soc 40:1361–1403. https://doi.org/10.1063/1.4929609

Li TQ, Henriksson U, Odberg L (1993) Determination of pore sizes in wood cellulose fibers by $^{2}H$ and $^{1}H$ NMR. Nord Pulp Pap Res J 8:326–330. https://doi.org/10.3183/npprj-1993-08-03-p326-330

Li X, Li Y, Chen C, Zhao D, Wang X, Zhao L, Shi H, Ma G, Su Z (2015) Pore size analysis from low field NMR spin–spin relaxation measurements of porous microspheres. J Porous Mater 22:11–20. https://doi.org/10.1007/s10934-014-9864-x

Lin JK, Ladisch MR, Patterson JA, Noller CH (1987) Determining pore size distribution in wet cellulose by measuring solute exclusion using a differential refractometer. Biotechnol Bioeng 29:976–981. https://doi.org/10.1002/bit.260290809

Meyer M, Buchmann C, Schaumann GE (2015) Determination of quantitative pore size distributions of soils with $^{1}H$-NMR Relaxometry. Eur J Soil Sci 69:393–406. https://doi.org/10.1111/ejss.12548

Murata K, Masuda M (2006) Microscopic observation of transverse swelling of latewood tracheid: effect of macroscopic/mesoscopic structure. J Wood Sci 52:283–289. https://doi.org/10.1007/s10086-005-0760-5

Penttilä PA, Rautkari L, Österberg M, Schweins R (2019) Small-angle scattering model for efficient characterization of wood nanostructure and moisture behaviour. J Appl Crystallogr 52:369–377. https://doi.org/10.1107/s1600576719002012

Penttilä PA, Altgen M, Carl N, Linden P, Morfin I, Österberg M, Schweins R, Rautkari L (2020) Moisture-related changes in the nanostructure of woods studied with X-ray and neutron scattering. Cellulose 27:71–87. https://doi.org/10.1007/s10570-019-02781-7

Provencher SW (1982) CONTIN: a general purpose constrained regularization program for inverting noisy linear algebraic and integral equations. Comput Phys Commun 27:229–242. https://doi.org/10.1016/0010-4655(82)90174-6

Stamm AJ (1967) Movement of fluids in wood-Part I: flow of fluids in wood. Wood Sci Technol 1:122–141. https://doi.org/10.1007/bf00353384

Toba K, Yamamoto H, Yoshida M (2012) Mechanical interaction between cellulose microfibrils and matrix substances in wood cell walls induced by repeated wet-and-dry treatment. Cellulose 19:1405–1412. https://doi.org/10.1007/s10570-012-9700-x

Toumelin E, Torres-Verdín C, Sun B, Dunn KJ (2007) Random-walk technique for simulating NMR measurements and 2D NMR maps of porous media with relaxing and permeable boundaries. J Magn Reson 188:83–96. https://doi.org/10.1016/j.jmr.2007.05.024

Viel S, Capitani D, Proietti N, Ziarelli F, Segre AL (2004) NMR spectroscopy applied to the cultural heritage: a preliminary study on ancient wood characterisation. Appl Phys A Mater Sci Process 79:357–361. https://doi.org/10.1007/s00339-004-2535-z

Vitas S, Segmehl J, Burgert I, Cabane E (2019) Porosity and pore size distribution of native and delignified beech wood determined by mercury intrusion porosimetry. Materials. https://doi.org/10.3390/ma12030416

Yang HS, Tze WTY (2017) Nitrogen adsorption analysis of wood saccharification residues. J Korean Wood Sci Technol 45:232–242. https://doi.org/10.5658/wood.2017.45.2.232

Yin J, Song K, Lu Y, Zhao G, Yin Y (2015) Comparison of changes in micropores and mesopores in the wood cell walls of sapwood and heartwood. Wood Sci Technol 49:987–1001. https://doi.org/10.1007/s00226-015-0741-9

Zabler S, Paris O, Burgert I, Fratzl P (2010) Moisture changes in the plant cell wall force cellulose crystallites to deform. J Struct Biol 171:133–141. https://doi.org/10.1016/j.jsb.2010.04.013